Charge Transfer into Organic Thin Films: A Deeper Insight through Machine-Learning-Assisted Structure Search

Alexander T. Egger, Lukas Hörmann, Andreas Jeindl, Michael Scherbela, Veronika Obersteiner, Milica Todorović, Patrick Rinke, and Oliver T. Hofmann*

Density functional theory calculations are combined with machine learning to investigate the coverage-dependent charge transfer at the tetracyanoethylene/Cu(111) hybrid organic/inorganic interface. The study finds two different monolayer phases, which exhibit a qualitatively different charge-transfer behavior. Our results refute previous theories of long-range charge transfer to molecules not in direct contact with the surface. Instead, they demonstrate that experimental evidence supports our hypothesis of a coverage-dependent structural reorientation of the first monolayer. Such phase transitions at interfaces may be more common than currently envisioned, beckoning a thorough reevaluation of organic/inorganic interfaces.

1. Introduction

One of the major factors governing device performance of organic electronic devices is the electronic level alignment between the organic material and the inorganic electrode.[1–3] Here, deviations from the Schottky–Mott limit (i.e., vacuum level alignment) are frequently observed due to the formation of interface dipoles.[1,4,5] Besides intramolecular bonds, the major contribution to dipole formation stems from adsorption-induced charge rearrangements, that is, charge transfer between the electrode and the organic material. The spatial extent of these charge rearrangements plays a key role for device performance: while very localized charge rearrangements cause an abrupt change

in the level positions at the interface, long-ranged charge transfer that extends beyond the layer in direct contact with the electrode leads to band bending.[6–10] Even if the band bending occurs only within the first few nm of the organic material, it reshapes and lowers charge-injection barriers,[11] thus affecting the performance of the whole device.[12]

While most surface science studies report interfacial charge transfer to be confined to the first monolayer of the organic film,[13–20] a few, sporadic, but recurrent reports observe interfacial charge transfer over longer distances, that is, to the second monolayer or beyond.[6–8,10,21,22] Given the relevance to device performance, it is important to investigate if long-range charge transfer is at all plausible, and if so, what governs the extent of the transferred charge? Conversely, if long-range charge transfer does not occur, what is then seen in the experiments?

To answer these questions, we study the interface between tetracyanoethylene (TCNE) and Cu(111). TCNE/Cu(111) arguably exhibits the strongest experimental indications for long-range charge transfer at an interface observed so far.[23–26] To gain microscopic insight into this interface, we carry out first-principles calculations for the TCNE/Cu(111) interface and combine them with two recent machine-learning-based advances, Bayesian Optimization Structure Search (BOSS)[27,28] and Surface Adsorbate polyMorph Prediction with Little Effort (SAMPLE).[29] The machine-learning augmentation proves crucial, as it allows us to harness the structural complexity of the organic/inorganic interface. Through it we show that even for this prototypical system, what appears to be charge transfer into higher layers is, in fact, a transition from flat-lying molecules to a more densely packed phase of upright-standing molecules, accompanied by a fundamental change of the charge-transfer interaction between substrate and adsorbate.

A. T. Egger, L. Hörmann, A. Jeindl, M. Scherbela, V. Obersteiner,
Prof. O. T. Hofmann
Institute of Solid State Physics
Graz University of Technology, NAWI Graz
Graz Petersgasse, 16/II 8010, Austria
E-mail: o.hofmann@tugraz.at
Dr. M. Todorović, Prof. P. Rinke
Department of Applied Physics
Aalto University School of Science
Aalto FI-00076, Finland

2. Previous Work on the TCNE/Cu Interface: The Situation Thus Far

A good experimental indicator for charge transfer to TCNE molecules at the TCNE/Cu interface is a change in the TCNE C=C stretch frequency, since the electron accepting lowest unoccupied molecular orbital (LUMO) is antibonding with respect to
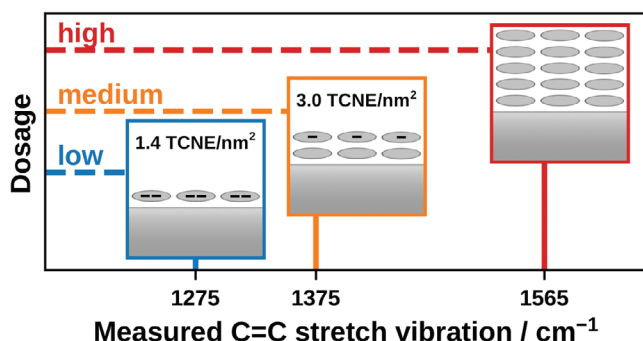
**ADVANCED
SCIENCE NEWS**

www.advancedsciencenews.com

**ADVANCED
SCIENCE**
Open Access

www.advancedscience.com

Figure 1. Measured C=C stretch vibration as function of TCNE deposition on Cu(111) and their interpretation by Erley and Ibach.[23]

Figure 2. Different building blocks for TCNE on Cu(111): (1–3) "lying": $E_{ads} = -1.87$ to -1.61 eV; (4–7) "standing": $E_{ads} = -1.65$ to -1.54 eV.

this bond. Erley and Ibach[23] measured the TCNE C=C stretch frequency as a function of the amount of deposited molecules using electron energy loss spectroscopy (EELS). As indicated in **Figure 1**, they observed a signal at 1275 cm^{-1} for a low coverage of 1.4 TCNE/nm^2, which they interpreted as multiply charged molecules in direct contact with the Cu surface. At an intermediate coverage of $\approx$3 TCNE/nm^2, a new vibrational feature appeared at 1375 cm^{-1}, which was interpreted as emergence of singly charged molecules in the second layer. Depositing even more molecules eventually gave rise to a new vibration at 1565 cm^{-1}, indicative of neutral molecules in the bulk. (For reference, the C=C vibration of an isolated TCNE molecule in the gas phase is 1509 cm^{-1}).

Theoretical models have been proposed to explain the emergence of long-ranged charge transfer. They are based either on electrostatic considerations and Fermi–Dirac statistics,[30] or on the presence of defects and disorder.[8] However, these models rely on prior assumptions and model parameters (e.g., a particular shape of the density of states). Furthermore, they do not provide the required insight into the atomistic and electronic structure at the interface, which is atomic to predict interface specific, experimental observables. Density functional theory (DFT) as the primary electronic structure theory method in materials science would, in principle, provide these details. However, despite the fact that the commonly applied PBE functional,[31] overestimates charge transfer,[32–34] pertinent studies do not support long-ranged charge transfer[35] nor are they able to explain the clear experimental indications for it.

We argue that this apparent failure of PBE is not due to its inherent limitations, but due to incorrect or insufficient structural models of the interface. The interface geometry used in first-principles calculations is typically based on educated guesses—also frequently referred to as chemical intuition—rather than the result of a comprehensive structure search. Despite advances in the computational structure prediction of organic crystals[36–42] and surface adsorbates,[28,29,43–45] computational structure determination is presently one of the most fundamental challenges for first-principles simulations. This is especially true for interfaces, for which the number of possible structures is large and the computational cost to evaluate their energy accurately is high.[36,37,46–48]
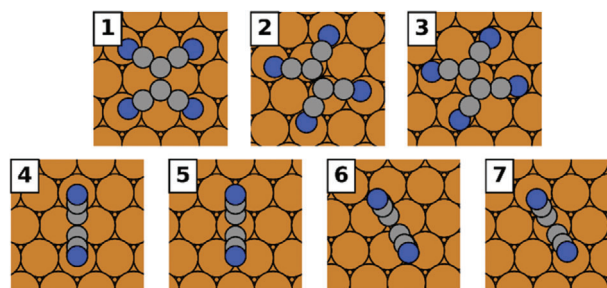
3. Addressing the TCNE/Cu Interfacial Structure Search Challenge

We address the structure search challenge by combining two recent machine-learning-based advances, BOSS[27,28] and SAMPLE.[29] These methods employ Bayesian optimization and Bayesian linear regression to learn complex potential energy surfaces (BOSS for individual molecules, SAMPLE for molecular layers) with only a few hundred energy evaluations. As will be shown in this work, our structural identification is central to solving the long-range charge-transfer puzzle for TCNE on copper.

All calculations in this study are performed with the PBE functional,[31] augmented with the TS^{surf} van der Waals correction[49] for interfaces as implemented in the FHI-aims[50] code. Since different structural polymorphs often have very similar energies,[51] we choose highly converged numerical settings, that yield DFT energies with an accuracy of 10 meV per molecule (for details see Supporting Information). We begin our study with the structure of the (sub)monolayer TCNE films on Cu(111), before proceeding to thin films. We determine the structure using the SAMPLE approach, which employs single molecule adsorbates as building blocks for assembling thin film polymorph candidates. The specifics of this procedure, including building block selection, are presented in ref. [29] and the Supporting Information.

We find seven plausible building blocks, that can be grouped into two categories, as shown in **Figure 2**. "Lying" TCNE molecules (blocks 1–3), in which all CN groups are in direct contact with the Cu substrate, are the energetically most favorable adsorption geometries ($E_{ads} = -1.87$ to -1.61 eV). "Standing" TCNE (4–7) (see Figure 2) molecules that touch the substrate with only two CN groups are the second class. A third category also exists (with a different orientation of the C=C bond with respect to the surface, see Supporting Information), but these molecules bind so weakly to the surface, that they do not play a role for the following discussion.

SAMPLE combinatorially combines these building blocks into polymorph candidates. We consider polymorphs with unit cells containing between one and three molecules corresponding to coverages between 0.5 and 5.0 TCNE/nm^2 to simulate the deposition of molecules in the experiment (and to allow for some experimental and theoretical error). Overall, this gives us a list of $\approx$10^7 possible structures. From these, we select a set of 300 structures according to the D-optimality criterion,[52] calculate their energy, and train our model. The quality of the trained model
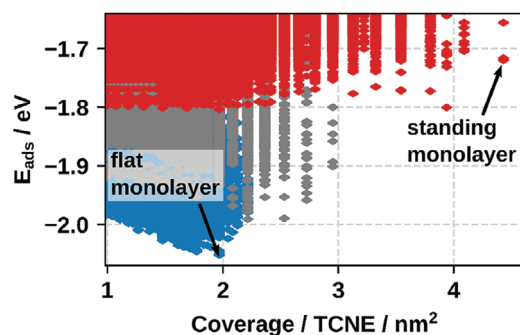
**ADVANCED
SCIENCE NEWS**

www.advancedsciencenews.com

**ADVANCED
SCIENCE**
Open Access

www.advancedscience.com

Figure 3. Predicted adsorption energies of all polymorph candidates; blue: polymorphs consisting of "lying" TCNE; red: "standing" TCNE; gray: mixed orientations.

is verified on 58 randomly drawn, previously unseen structures. We obtain an RMSE of 18 meV per molecule, which is small and in the same order of magnitude as the numerical convergence settings for our DFT calculations (details in Supporting Information).

While SAMPLE helps us to determine the submonolayer and monolayer morphologies, the configurational study of molecules adsorbing into the second layer presents a different challenge. The bilayer-forming molecular building blocks now have no well-defined adsorption sites on top of the first layer. We explore the complex potential energy surface (PES) of an additional molecule on the first layer using the BOSS approach for global structure search[27] (see Supporting Information for details). We then data mine the BOSS-PES to find local minima,[28] from which we launch PBE geometry optimizations to determine the energetically most favorable adsorption configurations for TCNE in the second layer (see Supporting Information for details).

4. Results: Structure of the TCNE/Cu Interface and its Implication on Charge Transfer

We first investigate submonolayer films. By definition, a submonolayer forms when the number of molecules is limited and the interface is not in thermodynamic equilibrium with a molecular reservoir. This corresponds to low molecular dosages in physical vapor deposition experiments. Under these circumstances, the molecules at the interface will assume the structure with the lowest energy per molecule (we define exothermic adsorption as negative, i.e., the lowest energy corresponds to the most stable structure). **Figure 3** shows the predicted energies for the different polymorphs as function of their coverage. We find that structures that contain exclusively flat-lying molecules (blue points in Figure 3) yield more favorable energies per molecule than those that contain upright-standing moieties.

Because TCNE has four peripheral, negatively charged CN groups, one might expect that the molecules repel each other in analogy to the prototypical F4TCNQ molecule.[53] If that was indeed the case, the lowest coverage would have the most negative adsorption energy. However, as Figure 3 shows, increasing the coverage systematically lowers the adsorption energy between 1 and 2 TCNE/nm² before tighter packing leads to an inevitable energy increase due to Pauli repulsion. This trend demonstrates
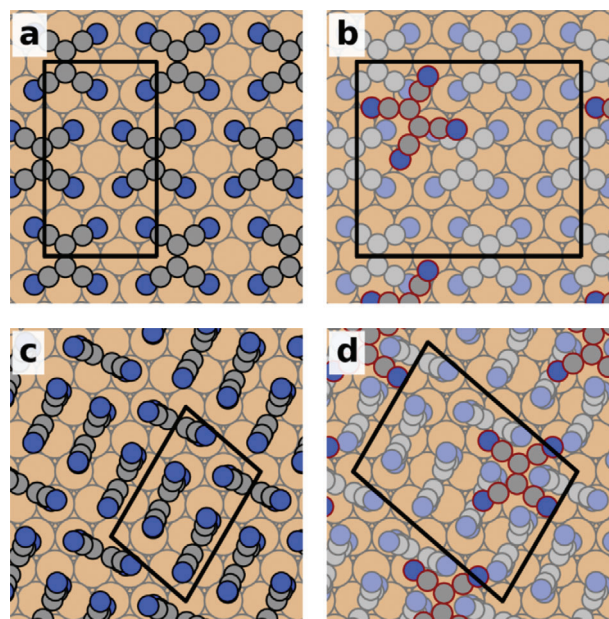

Figure 4. Optimized structures for the a) flat (sub)monolayer, b) flat monolayer with an additional molecule in second layer ('flat-on-flat'), c) standing monolayer, d) standing monolayer with additional molecule in second layer ('flat-on-standing").

that there are, in fact, dominant intermolecular interactions that are attractive. It furthermore indicates that islands are likely to form, which grow until the whole substrate is covered and a closed (mono)layer will be formed. The experiments for low coverage in ref. [23] should hence be compared to a close-packed structure, not to individual molecules.

From our results, the best candidate for the submonolayer structure is the energetically most favorable polymorph (see **Figure 4**a) observed at a coverage of 1.97 TCNE/nm². This coverage is ≈40% more dense than the experimentally reported value for the closure of the first monolayer (1.4 TCNE/nm²).[23] We tentatively attribute this discrepancy to a systematic overestimation of the coverage in experiment, as discussed below and, in more detail, in the Supporting Information. The energetically most favorable structure comprises two non-equivalent, flat-lying TCNE molecules that are slightly offset with respect to each other such that the (negatively charged) cyano groups point toward the (more positive) central C=C region. A structural representation is shown in the Supporting Information. While there are several energetically similar polymorphs (20 structures are within 18 meV, the RMSE of our model), it is important to emphasize that all of them a) have the same, or a very similar, coverage and b) contain only flat-lying molecules.

To validate the low-coverage structure shown in Figure 4a, we determined its electronic structure and vibrational spectrum (for methodological details see Supporting Information). We find that the TCNE molecules exhibit a (Mulliken) charge of only ≈0.1 electrons, that is, they are basically charge neutral, at variance with the reported "multiply charged" molecules in ref. [23]. The reason for this is that TCNE, just like its cousins TCNQ[54] and F4TCNQ,[55,56] exhibits a Blyholder-like[57] charge-transfer mechanism. The Cu substrate donates ≈1.6 electrons into the

**ADVANCED
SCIENCE NEWS**

www.advancedsciencenews.com

**ADVANCED
SCIENCE**
Open Access

www.advancedscience.com

molecular LUMO, while TCNE concurrently backdonates ≈1.4 electrons to Cu. Although the molecule is overall charge neutral, the experimentally examined C=C stretch vibration is only sensitive to the charge in the TCNE LUMO. This is because the LUMO is antibonding with respect to the C=C bond, that is, filling the LUMO weakens this bond and shifts its frequency to lower wavenumbers. Conversely, the backdonation occurs through the CN groups (see Supporting Information), which are non-bonding with respect to the central C=C bond, and thus do not affect the C=C stretch vibration.

The structure contains two non-equivalent molecules in the unit cell, whose computed C=C stretch vibrations in the unit cell are 1236 and 1240 cm^{-1}, in favorable agreement with the experimental low-coverage value of 1275 cm^{-1}. (For comparison, the C=C vibration of the neutral, isolated TCNE molecule is found at 1509 cm^{-1} in the gas phase and at 1585 cm^{-1} in the bulk). Although a discrepancy of 40 cm^{-1} may appear large, we note that PBE generally underbinds[32] and overestimates the charge transfer.[32–34] Both effects lead to a too weak C=C bond, so a deviation from experiment in this order of magnitude is to be expected. Thus, our study so far corroborates the observed large charge transfer that occurs in direct contact of TCNE with the metal, even if the mechanism is more involved than originally envisioned.

Having established that TCNE forms dense islands that grow until a monolayer is formed, we increase the dosage by predicting the structure of further deposited molecules. Presumably, these would go into the second layer. As first approximation, we assume that the first layer does not rearrange, and explore the energetics of a single, isolated molecule on top of it. Here, the BOSS tool for global structure search allows us to identify the preferred molecular configuration (see Supporting Information for details). We find that TCNE adsorbs with its π-plane parallel to the surface, that is, flat lying on top of the flat-lying first monolayer. This maximizes the van der Waals interaction, while minimizing the wave function overlap (and hence Pauli repulsion) with the first layer. We will refer to this geometry, shown in Figure 4b, as "flat-on-flat" hereafter. In passing, we note that on metals, sometimes growth modes are observed where the second layer adsorbs upright on a flat-lying "wetting' layer.[58] However, this appears not to be the case here.

The "flat-on-flat" geometry features a minute charge transfer (≈0.2 e) to the molecule in the second layer, which could indicate long-ranged charge transfer. As the corresponding density of states shows (see Supporting Information), this charge transfer is triggered by hybridization of the LUMO of the TCNE molecule in the second layer with the (filled) LUMO of TCNE in the first layer. Vibrational analysis shows that the C=C stretch vibrations for these molecules are located at 1458 cm^{-1}. However, this result matches neither the observed peak at 1375 cm^{-1} nor the one at 1565 cm^{-1}, indicating that this geometry does not appear experimentally. This discrepancy cannot be explained by the flaws of our computational method (PBE). We thus must conclude that the "flat-on-flat" second layer geometry does not form in experiment, and reconsider the structure of the full monolayer.

Ultimately, upon depositing ever more molecules, solid bulk TCNE will form. In contrast to the submonolayer regime, this constitutes a reservoir with which the thin film is in contact. (Ab
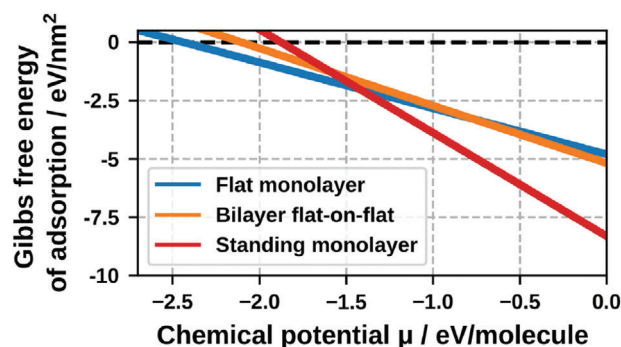

Figure 5. Gibbs free energy of adsorption for different polymorphs as function of the chemical potential, μ.

initio) thermodynamics[59] then stipulates that the favored structure must minimize the Gibbs energy per area

$$\gamma = \frac{1}{A}\left(\Delta E - TS + pV + F_{vib} - \Delta\mu(p, T) \cdot N\right) \qquad (1)$$

where ΔE is the adsorption energy per molecule (as obtained by DFT), N the number of molecules per unit cell with area A, and μ the chemical potential of the reservoir. μ controls the transition between the complete absence of a reservoir (low μ) and the formation of bulk TCNE (at large chemical potentials), that is, increasing μ corresponds to increasing molecular dosage. We note that μ could also be expressed as pressure and temperature of a TCNE gas reservoir. We provide a corresponding phase diagram, together with a critical discussion how it relates to the present experiment, in the Supporting Information. In the equation above, the work term (pV) and the configurational entropy (TS) are usually small and thus neglected, as commonly done in the literature.[59] The vibrational enthalpy (F_{vib}) can be substantial, if the interaction with the substrate differs substantially.[60] Therefore, we include the zero-point energy in this consideration, but neglect its temperature dependence (i.e., the thermal occupation of vibrations), as its differences between different polymorphs (which govern their relative stability) are very small.

Equation (1) allows us to recast the energies of all determined polymorphs into analytical functions of the chemical potential. **Figure 5** illustrates the results for the polymorphs with the lowest Gibbs free energy. The predicted submonolayer (lying TCNE molecules, blue line) is the thermodynamically stable structure at low μ. At $\mu = -1.43$ eV, the more densely packed polymorph shown in Figure 4c becomes more favorable (see red line in Figure 5). This structure, the "standing monolayer," is shown in Figure 4c and consists of upright-standing molecules in the first layer with a coverage of 4.43 TCNE/nm^2. It shows an arrangement of lines of slip-stacked molecules that are separated by molecules rotated (almost) 90 degrees to them, that is, a combination of π-stacking with a herringbone-like pattern. Interestingly, (in energy per area) this structure is significantly more favorable than any other polymorph, the next candidate being ≈250 meV/nm^2 worse in energy. Importantly, all structures with low energies per area contain exclusively upright-standing molecules, in salient contrast to the energy per molecule, for which all energetically favorable structures contain exclusively flat-lying molecules. Importantly, none of the other monolayer

polymorphs ever exhibit a lower γ than these two structures at any μ, indicating a phase transition from flat-lying to upright-standing molecules upon increasing dosage (provided the flat-lying polymorph is not kinetically trapped).

We find that the "flat-on-flat" bilayer geometry is never a minimum in γ, either. Rather, it is energetically more favorable to include another molecule into the first layer, and rearrange the molecules from flat lying to upright standing, before placing even a single molecule in the second layer. (Specifically, the flat-on-flat bilayer is 230 meV per molecule less stable than the standing monolayer, which is ten times more than our model uncertainty.)

From these results it becomes clear that we need to consider a monolayer of standing molecules before we can analyze the potential charge transfer to molecules in the second layer. We note that the coverage of the upright-standing monolayer is again ≈40% more dense than the coverage reported for the maximum of the 1375 cm^{-1} peak in the experiment.[23] The fact that we overestimate the density of both the flat-lying and the upright-standing monolayer by the same factor corroborates our tentative explanation of a systematic error in the experimental determination of the coverage (since most other explanations would require random errors to be the same, which is unlikely).

The electronic structure for a monolayer of upright-standing molecules shows that the molecules are essentially neutral with an average net charge of 0.06 e. There is still substantial charge transfer at the interface, originating from a charge donation of ≈0.8 electrons into the LUMO and a backdonation of 0.95 electrons from the two CN groups in contact with the surface. The C=C stretch vibrations for three upright-standing molecules in the unit cell are at 1318, 1349, and 1357 cm^{-1}, respectively, which is in good agreement with the experimentally determined value at intermediate coverage (1375 cm^{-1}). This authenticates our finding of a phase transition in the first layer. It furthermore shows that the experimental indication for long-range charge transfer, formally assigned to singly charged molecules in the second layer, in fact stems from (conventional) short-ranged charge transfer into molecules in direct contact with the surface. In hindsight, this conclusion is corroborated experimentally. To complement their EELS results,[23] Erley later investigated the same system using infra-red (IR) spectroscopy.[24] There, they found no indication of the C=C strech vibration at low coverage, but observesd a strong signal at intermediate coverage. Contrary to EELS, IR is sensitive to the molecular orientation. For any flat-lying TCNE, the IR-active transition dipole moment of the C=C vibration would be screened out by the opposing metal surface mirror dipole. In the upright-standing molecules, the signal was amplified by the same mechanism, producing the experimental observation.

Since the flat-on-flat bilayer geometry did show indications of long-range charge transfer, we carefully checked whether this behavior persists for TCNE adsorbed on the upright-standing monolayer. Again, we use BOSS to determine the geometry of an additional molecule in the second layer (see Figure 4d). We find that on the upright-standing monolayer, the most stable geometry in the second layer consists of basically flat-lying TCNE molecules, see Supporting Information. Hence, we call it "flat-on-standing" hereafter. In contrast to the flat-on-flat geometry, here molecules in the second layer remain charge-neutral (Mulliken charge: 0.02 electrons), that is, there is no notable long-range charge transfer for this structure. The C=C stretch vibration is at 1513 cm^{-1}, in qualitative agreement with the experimental value of 1565 cm^{-1}. Evaluating γ for this structure shows that it becomes stable only at very high μ (>-0.5 eV), as shown in the Supporting Information. This indicates that there is only a very small window in which a bilayer will be observed before bulk TCNE forms. Evaluating the stretch vibration for bulk TCNE (as taken from the Cambridge Structural Database) yields the C=C stretch vibration at 1585 cm^{-1}, which now fits the measured value very well.

5. Temperature Effects and Constraints of Our Search Space

As a minor caveat, we note that it was not technically possible to include surface adatoms in this work. Many metal/organic interfaces contain surface adatoms,[3,61–63] including TCNE on Cu(100).[64] The experimental underestimation of the packing density here might be taken as an indication of adatoms. Still, there are several arguments against this hypothesis. The experimental study was performed on the closely packed Cu(111) surface (fewer adatoms available), with TCNE deposited at 100 K, further reducing the availability of adatoms. Structurally, adatoms strongly reduce the bending of the adsorbate[61] and thereby decrease the metal-to-adsorbate charge transfer,[65] which is inconsistent with the experimental findings. Thus, the good agreement between computed and experimental observables additionally suggests that surface adatoms are not relevant for the present system.

Also the fact that we have neglected temperature effects deserves further scrutiny. Finite temperature affects the free energy landscape through various factors. First, vibrations become thermally occupied according to Bose–Einstein statistics. Because TCNE/Cu consists mostly of rigid bonds, it exhibits mostly high-energy vibrations, that are almost completely in their ground state at $T < 300$ K. Thus, while it is important to account for the energy contributions arising from the shift of the zero-point vibrations, the thermal occupation of the vibrations can be safely neglected. The second effect is the configurational entropy. As shown in the Supporting Information, the configurational entropy is the same for all polymorphs of a given coverage, and between different coverages, it changes by ≈0.5 meV per adsorption site (at 300 K), or ≈$0.3 k_B T$ per nm^2. A comparison with Figure 3 shows that this is several orders of magnitude smaller than the change of the adsorption energy. Thus, also the configuration entropy can be safely neglected. Finally, at finite temperature several polymorphs could co-exist on the surface, populated according to Boltzmann statistics. This may be particularly relevant for the flat-lying polymorph, where we find multiple structures with similar energies just outside our numerical accuracy. However, it is important to emphasize that all structures in the submonolayer regime are flat lying, and exhibit similar vibrational frequencies (since this mostly depends on the charge state, which itself depends on whether the molecules lie down or stand upright). Even if there is a co-existence of multiple flat-lying polymorphs with different geometries in the submonolayer regime, the predicted flat-lying to upright-standing phase transition would still occur.

**ADVANCED
SCIENCE NEWS**

www.advancedsciencenews.com

**ADVANCED
SCIENCE**
Open Access

www.advancedscience.com

Table 1. Computationally determined thermodynamically stable structures, their C=C stretch frequencies ν, overall charge Q and LUMO occupation f.

Structure	ν [cm]	Q (electrons)	f (electrons)
Flat monolayer	1236, 1240	0.1	1.6
Standing monolayer	1318, 1349, 1357	−0.1	1.2
Flat-on-standing	1513	≈0.0	≈0

6. Conclusion

In summary, for TCNE on Cu(111) our study refutes the notion of long-range charge transfer beyond the first layer. We find instead that at increasing coverage, the TCNE monolayer undergoes a phase transition from a flat-lying geometry to an upright-standing phase on the substrate. The flat-lying molecules are overall charge neutral, but significant short-range charge donation and backdonation result in an almost doubly occupied LUMO. The upright-standing molecules are also neutral, but the different charge rearrangements lead to only ≈1 electron in the (former) LUMO. Further, molecules deposited onto this structure start to adsorb in the second layer, and remain charge neutral with no charge donation or backdonation from the substrate or molecules below.

Our structural predictions are substantiated by the good agreement between measured and computed C=C stretch vibrations, as shown in **Table 1**. Similar phase transitions of the first layer have been found also for other systems,[66–70] usually based on experimental evidence. Molecular dynamics simulations also successfully predict coverage-dependent reorientations for physisorbed systems,[71–73] but force fields struggle with the formation and breaking of partially covalent bonds (such as the CN–Cu bond) and the different charge distributions found in the present system. The first-principles based approach used in this work provides complementary insight into more strongly interacting, electronically more complicated systems, although at the cost of being unable to give energetic barriers or phase transformation timescales.[66–70]

Our calculations show that charge transfer into the second layer does occur in certain molecular arrangements (see the flat-on-flat geometry), which are unstable here. We therefore propose that structural changes at metal/organic interfaces triggered by increasing coverage may be more common than previously thought. This finding highlights the importance of determining the atomic structure at interfaces, and the significance of contemporary first-principles calculations combined with machine learning in helping to understand experimental observations.

Supporting Information

Supporting Information is available from the Wiley Online Library or from the author.

Conflict of Interest

The authors declare no conflict of interest.

[1] H. Ishii, K. Sugiyama, E. Ito, K. Seki, *Adv. Mater.* **1999**, *11*, 605.
[2] N. Koch, *ChemPhysChem* **2007**, *8*, 1438.
[3] R. Otero, A. V. de Parga, J. M. Gallego, *Surf. Sci. Rep.* **2017**, *72*, 105.
[4] S. Braun, W. Osikowicz, Y. Wang, W. R. Salaneck, *Org. Electron.* **2007**, *8*, 14.
[5] E. Zojer, T. C. Taucher, O. T. Hofmann, *Adv. Mater. Interfaces* **2019**, *6*, 1900581.
[6] I. Lange, J. C. Blakesley, J. Frisch, A. Vollmer, N. Koch, D. Neher, *Phys. Rev. Lett.* **2011**, *106*, 216402.
[7] J. Hwang, E.-G. Kim, J. Liu, J.-L. Bredas, A. Duggal, A. Kahn, *J. Phys. Chem. C* **2007**, *111*, 1378.
[8] G. Paasch, H. Peisert, M. Knupfer, J. Fink, S. Scheinert, *J. Appl. Phys.* **2003**, *93*, 6084.
[9] H. Ishii, N. Hayashi, E. Ito, Y. Washizu, K. Sugi, Y. Kimura, M. Niwano, Y. Ouchi, K. Seki, *Phys. Status Solidi A* **2004**, *201*, 1075.
[10] R. Schlaf, P. Schroeder, M. Nelson, B. Parkinson, P. Lee, K. Nebesny, N. R. Armstrong, *J. Appl. Phys.* **1999**, *86*, 1499.
[11] K. Zojer, T. Rothländer, J. Kraxner, R. Schmied, U. Palfinger, H. Plank, W. Grogger, A. Haase, H. Gold, B. Stadlober, *Sci. Rep.* **2016**, *6*, 31387.
[12] F. Neumann, Y. A. Genenko, C. Melzer, S. Yampolskii, H. von Seggern, *Phys. Rev. B* **2007**, *75*, 205322.
[13] S. Winkler, J. Frisch, R. Schlesinger, M. Oehzelt, R. Rieger, J. Räder, J. P. Rabe, K. Müllen, N. Koch, *J. Phys. Chem. C* **2013**, *117*, 22285.
[14] N. Koch, S. Duhm, J. P. Rabe, A. Vollmer, R. L. Johnson, *Phys. Rev. Lett.* **2005**, *95*, 237601.
[15] B. J. Topham, M. Kumar, Z. G. Soos, *Adv. Funct. Mater.* **2011**, *21*, 1931.
[16] A. Alkauskas, L. Ramoino, S. Schintke, M. von Arx, A. Baratoff, H.-J. Güntherodt, T. Jung, *J. Phys. Chem. B* **2005**, *109*, 23558.
[17] P. Gargiani, M. Angelucci, C. Mariani, M. G. Betti, *Phys. Rev. B* **2010**, *81*, 085412.
[18] I. Hill, A. Rajagopal, A. Kahn, *J. Appl. Phys.* **1998**, *84*, 3236.
[19] W. Gao, A. Kahn, *J. Appl. Phys.* **2003**, *94*, 359.
[20] G. Brocks, D. Çakır, M. Bokdam, M. P. de Jong, M. Fahlman, *Org. Electron.* **2012**, *13*, 1793.
[21] I. Kröger, B. Stadtmüller, C. Kumpf, *New J. Phys.* **2016**, *18*, 113022.
[22] R. Forker, C. Golnik, G. Pizzi, T. Dienel, T. Fritz, *Org. Electron.* **2009**, *10*, 1448.
[23] W. Erley, H. Ibach, *J. Phys. Chem.* **1987**, *91*, 2947.

[24] W. Erley, *J. Phys. Chem.* **1987**, *91*, 6092.

[25] W. Erley, *J Electron Spectros. Relat. Phenomena* **1987**, *44*, 65.

[26] F. M. Pan, J. C. Hemminger, S. Ushioda, *J. Phys. Chem.* **1985**, *89*, 862.

[27] *Bayesian Optimization Structure Search (BOSS)*, https://cest.aalto.fi/boss.

[28] M. Todorović, M. U. Gutmann, J. Corander, P. Rinke, *NPJ Comput. Mater.* **2019**, *5*, 35.

[29] L. Hörmann, A. Jeindl, A. T. Egger, M. Scherbela, O. T. Hofmann, *Comput. Phys. Commun.* **2019**, *244*, 143.

[30] M. Oehzelt, N. Koch, G. Heimel, *Nat. Commun.* **2014**, *5*, 4174.

[31] J. P. Perdew, K. Burke, M. Ernzerhof, *Phys. Rev. Lett.* **1996**, *77*, 3865.

[32] J. P. Perdew, A. Ruzsinszky, L. A. Constantin, J. Sun, G. I. Csonka, *J. Chem. Theory Comput.* **2009**, *5*, 902.

[33] V. Atalla, M. Yoon, F. Caruso, P. Rinke, M. Scheffler, *Phys. Rev. B* **2013**, *88*, 165122.

[34] E. Kraisler, L. Kronik, *Phys. Rev. Lett.* **2013**, *110*, 126403.

[35] H. Wang, S. V. Levchenko, T. Schultz, N. Koch, M. Scheffler, M. Rossi, *Adv. Electron. Mater.* **2019**, *5*, 1800891.

[36] S. L. Price, *Chem. Soc. Rev.* **2014**, *43*, 2098.

[37] A. M. Reilly, R. I. Cooper, C. S. Adjiman, S. Bhattacharya, A. D. Boese, J. G. Brandenburg, P. J. Bygrave, R. Bylsma, J. E. Campbell, R. Car, D. H. Case, R. Chadha, J. C. Cole, K. Cosburn, H. M. Cuppen, F. Curtis, G. M. Day, R. A. DiStasio, Jr, A. Dzyabchenko, B. P. van Eijck, D. M. Elking, J. A. van den Ende, J. C. Facelli, M. B. Ferraro, L. Fusti-Molnar, C.-A. Gatsiou, T. S. Gee, R. de Gelder, L. M. Ghiringhelli, H. Goto, et al. *Acta Crystallogr. B. Struct. Sci. Cryst. Eng. Mater.* **2016**, *72*, 439.

[38] A. M. Reilly, A. Tkatchenko, *J. Phys. Chem. Lett.* **2013**, *4*, 1028.

[39] F. Curtis, X. Li, T. Rose, A. Vazquez-Mayagoitia, S. Bhattacharya, L. M. Ghiringhelli, N. Marom, *J. Chem. Theory Comput.* **2018**, *14*, 2246.

[40] D. McDonagh, C.-K. Skylaris, G. M. Day, *J. Chem. Theory Comput.* **2019**, *15*, 2743.

[41] J. G. Brandenburg, S. Grimme, *J. Phys. Chem. Lett.* **2014**, *5*, 1785.

[42] S. M. Woodley, R. Catlow, *Nat. Mater* **2008**, *7*, 937.

[43] D. M. Packwood, P. Han, T. Hitosugi, *Nat. Commun.* **2017**, *8*, 14463.

[44] D. M. Packwood, T. Hitosugi, *Appl. Phys. Express* **2017**, *10*, 065502.

[45] K. Krautgasser, C. Panosetti, D. Palagin, K. Reuter, R. J. Maurer, *J. Chem. Phys.* **2016**, *145*, 084117.

[46] A. R. Oganov, C. J. Pickard, Q. Zhu, R. J. Needs, *Nat. Rev. Mater.* **2019**, *4*, 331.

[47] J. K. Nørskov, T. Bligaard, J. Rossmeisl, C. H. Christensen, *Nat. Chem.* **2009**, *1*, 37.

[48] C. J. Pickard, R. Needs, *J. Phys. Condens. Matter* **2011**, *23*, 053201.

[49] V. G. Ruiz, W. Liu, E. Zojer, M. Scheffler, A. Tkatchenko, *Phys. Rev. Lett.* **2012**, *108*, 146103.

[50] V. Blum, R. Gehrke, F. Hanke, P. Havu, V. Havu, X. Ren, K. Reuter, M. Scheffler, *Comput. Phys. Commun.* **2009**, *180*, 2175.

[51] J. Nyman, G. M. Day, *CrystEngComm* **2015**, *17*, 5154.

[52] A. Atkinson, A. Donev, R. Tobias, *Optimum Experimental Designs, with SAS*, Vol. 34. Oxford University Press, Oxford **2007**.

[53] H.-Z. Tsai, A. A. Omrani, S. Coh, H. Oh, S. Wickenburg, Y.-W. Son, D. Wong, A. Riss, H. S. Jung, G. D. Nguyen, G. F. Rodgers, A. S. Aikawa, T. Taniguchi, K. Watanabe, A. Zettl, S. G. Louie, J. Lu, M. L. Cohen, M. F. Crommie, *ACS Nano* **2015**, *9*, 12168.

[54] T.-C. Tseng, C. Urban, Y. Wang, R. Otero, S. L. Tait, M. Alcamí, D. Écija, M. Trelka, J. M. Gallego, N. Lin, M. Konuma, U. Starke, A. Nefedov, A. Langner, C. Wöll, M. A. Herranz, F. Martín, N. Martín, K. Kern, R. Miranda, *Nat. Chem.* **2010**, *2*, 374.

[55] L. Romaner, G. Heimel, J.-L. Brédas, A. Gerlach, F. Schreiber, R. L. Johnson, J. Zegenhagen, S. Duhm, N. Koch, E. Zojer, *Phys. Rev. Lett.* **2007**, *99*, 256801.

[56] G. M. Rangger, O. T. Hofmann, L. Romaner, G. Heimel, B. Bröker, R.-P. Blum, R. L. Johnson, N. Koch, E. Zojer, *Phys. Rev. B* **2009**, *79*, 165306.

[57] G. Blyholder, *J. Phys. Chem.* **1964**, *68*, 2772.

[58] D. Käfer, L. Ruppel, G. Witte, *Physical Review B* **2007**, *75*, 085309.

[59] K. Reuter, M. Scheffler, *Phys. Rev. B* **2001**, *65*, 035406.

[60] H. Edlbauer, E. Zojer, O. T. Hofmann, *J. Phys. Chem. C* **2015**, *119*, 27162.

[61] P. Blowey, S. Velari, L. Rochford, D. Duncan, D. Warr, T.-L. Lee, A. De Vita, G. Costantini, D. Woodruff, *Nanoscale* **2018**, *10*, 14984.

[62] M. N. Faraggi, N. Jiang, N. Gonzalez-Lakunza, A. Langner, S. Stepanow, K. Kern, A. Arnau, *J. Phys. Chem. C* **2012**, *116*, 24558.

[63] P. Maksymovych, O. Voznyy, D. B. Dougherty, D. C. Sorescu, J. T. Yates, Jr, *Prog. Surf. Sci.* **2010**, *85*, 206.

[64] D. Wegner, R. Yamachika, Y. Wang, V. W. Brar, B. M. Bartlett, J. R. Long, M. F. Crommie, *Nano Lett.* **2008**, *8*, 131.

[65] O. T. Hofmann, D. A. Egger, E. Zojer, *Nano Lett.* **2010**, *10*, 4369.

[66] B. Bröker, O. Hofmann, G. Rangger, P. Frank, R.-P. Blum, R. Rieger, L. Venema, A. Vollmer, K. Müllen, J. Rabe, A. Winkler, P. Rudolf, E. Zojer, N. Koch, *Phys. Rev. Lett.* **2010**, *104*, 246805.

[67] K. Medjanik, D. Kutnyakhov, S. Nepijko, G. Schönhense, S. Naghavi, V. Alijani, C. Felser, N. Koch, R. Rieger, M. Baumgarten, K. Müllen, *Phys. Chem. Chem. Phys.* **2010**, *12*, 7184.

[68] C. Christodoulou, A. Giannakopoulos, M. Nardi, G. Ligorio, M. Oehzelt, L. Chen, L. Pasquali, M. Timpel, A. Giglia, S. Nannarone, P. Norman, M. Linares, K. Parvez, K. Müllen, D. Beljonne, N. Koch, *J. Phys. Chem. C* **2014**, *118*, 4784.

[69] A. Navarro-Quezada, E. Ghanbari, T. Wagner, P. Zeppenfeld, *J. Phys. Chem. C* **2018**, *122*, 12704.

[70] S. Kowarik, A. Gerlach, S. Sellner, F. Schreiber, L. Cavalcanti, O. Konovalov, *Phys. Rev. Lett.* **2006**, *96*, 125504.

[71] L. Muccioli, G. D'Avino, C. Zannoni, *Adv. Mater.* **2011**, *23*, 4531.

[72] S. Chen, J. Ma, *J. Chem. Phys.* **2012**, *137*, 074708.

[73] G. D'Avino, L. Muccioli, C. Zannoni, *Adv. Funct. Mater.* **2015**, *25*, 1985.

2000992 (7 of 7)